Lipid Recycling between the Plasma Membrane and Intracellular Compartments: Transport and Metabolism of Fluorescent Sphingomyelin Analogues in Cultured Fibroblasts

Michael Koval and Richard E. Pagano

Department of Embryology, Carnegie Institution of Washington, Baltimore, Maryland 21210-3301

Abstract. We examined the metabolism and intracellular transport of the D-*erythro* and L-*threo* stereoisomers of a fluorescent analogue of sphingomyelin, *N*-(*N*-[6-[(7-nitrobenz-2-oxa-1,3-diazol-4-yl)amino] caproyl])-sphingosylphosphorylcholine (C_6-NBD-SM), in Chinese hamster ovary (CHO-K1) fibroblast monolayers. C_6-NBD-SM was integrated into the plasma membrane bilayer by transfer of C_6-NBD-SM monomers from liposomes to cells at 7°C. The cells were washed, and within 10–15 min of being warmed to 37°C, C_6-NBD-SM was internalized from the plasma membrane to a perinuclear location that colocalized with the centriole and was distinct from the lysosomes and the Golgi apparatus. This perinuclear region was also labeled by internalized rhodamine-conjugated transferrin. C_6-NBD-SM endocytosis was not inhibited when the microtubules were disrupted with nocodazole; rather, the fluorescent lipid was distributed in vesicles throughout the cell periphery instead of being internalized to the perinuclear region of the cell. The metabolism of C_6-NBD-SM to other fluorescent sphingolipids at 37°C and its effect on C_6-NBD-SM transport was also examined.

To study plasma membrane lipid recycling, C_6-NBD-SM was first inserted into the plasma membrane of CHO-K1 cells and then allowed to be internalized by the cells at 37°C. Any C_6-NBD-SM remaining at the plasma membrane was then removed by incubation with nonfluorescent liposomes at 7°C, leaving cells containing only internalized fluorescent lipid. The return of C_6-NBD-SM to the plasma membrane from intracellular compartments upon further 37°C incubation was then observed. The half-time for a complete round C_6-NBD-SM recycling between the plasma membrane and intracellular compartments was ~40 min. Pretreatment of cells with either monensin or nocodazole did not inhibit C_6-NBD-SM recycling.

RECYCLING of plasma membrane receptors is a process involving membrane vesicle budding, fusion/fission and transport (10, 38). Since intracellular vesicles are involved in all known steps of the recycling process, there should also be considerable lipid transport in conjunction with protein recycling. However, no direct evidence for plasma membrane lipid recycling between intracellular compartments and the cell surface is available.

Previous work in our laboratory used fluorescent acyl chain-labeled glycerolipids as probes for studying endocytosis in cultured cells (32, 37). However, these probes are not practical for studies of lipid recycling because such studies require prolonged incubations at 37°C during which the fluorescent glycerolipids are extensively hydrolyzed by cellular phospholipases, releasing fluorescent fatty acid (37). Since sphingomyelin (SM)[1] is a major lipid constituent of the plasma membrane that is highly resistant to acyl chain hydrolysis (1), we have used a fluorescent analog of SM, *N*-(*N*-[6-[(7-nitrobenz-2-oxa-1,3-diazol-4-yl) amino]caproyl])-sphingosylphosphorylcholine (C_6-NBD-SM), to circumvent this problem in the present study. Using Chinese hamster ovary fibroblast cell line (CHO-K1) cells, we examined the internalization of this fluorescent lipid from the plasma membrane to intracellular compartments, and its subsequent return to the plasma membrane ("recycling") with time. We also studied the effect of SM stereochemistry on its metabolism and intracellular transport using stereoisomers of C_6-NBD-SM corresponding to the natural D-*erythro* or nonnatural L-*threo* forms of SM. Finally, the patterns of intracellular labeling obtained with C_6-NBD-SM were compared to those of a recycling protein to learn whether the same compartments are involved in lipid and protein recycling.

This work is in partial fulfillment of the requirements for a doctoral degree by M. Koval in the Department of Biology, The Johns Hopkins University, Baltimore, MD.

1. *Abbreviations used in this paper*: Cer, ceramide; CHO-K1, Chinese hamster ovary fibroblast cell line; DOPC, dioleoylphosphatidylcholine; GlcCer, glucosylceramide; HCMF, 10 mM Hepes-buffered calcium and magnesium-free Puck's saline, pH 7.4; HMEM, Hepes-buffered MEM; LUVET, large unilamellar vesicle by extrusion techniques; C_6-NBD, *N*-[6-[(7-nitrobenz-2-oxa-1,3-diazol-4-yl)amino]caproyl]; C_6-NBD-Cer, *N*-(C_6-NBD)-sphingosine; C_6-NBD-GlcCer, *N*-(C_6-NBD)-glucosylsphingosine; C_6-NBD-SM, *N*-(C_6-NBD)-sphingosylphosphorylcholine; Rh, rhodamine; Rh-Tf, Rh-conjugated transferrin; SM, sphingomyelin; SRh, sulforhodamine; SUV, small unilamellar vesicle.

Materials and Methods

Materials

Dioleoylphosphatidylcholine (DOPC) and dioleoylphosphatidylethanolamine were obtained from Avanti Polar Lipids, Inc. (Birmingham, AL). C_6-NBD-aminohexanoic acid, sulforhodamine chloride and sulforhodamine dextran, 10 kD (SRh-dextran) were purchased from Molecular Probes Inc. (Eugene, OR). Sodium cacodylate was from Electron Microscopy Sciences (Fort Washington, PA). Triphenylphosphine was from Aldrich Chemical Co. (Milwaukee, WI). All organic solvents were purchased from Burdick & Jackson Laboratories Inc. (Muskegon, MI). Rhodamine(Rh)-conjugated second antibodies were from Organon Teknika-Cappel (West Chester, PA). Rh-conjugated *Ricinus communis* agglutinin 120 was purchased from Vector Laboratories, Inc. (Burlingame, CA). Unless otherwise stated, all other materials were obtained from Sigma Chemical Co. (St. Louis, MO).

Cell Culture

Monolayer cultures of CHO-K1 fibroblasts (CCL 61; American Type Culture Collection, Rockville, MD) were grown in MEM Alpha medium (No. 410-2000; Gibco Laboratories, Grand Island, NY) supplemented with 5% FBS in a water-saturated atmosphere of 5% CO_2 in air. Cells were grown for 48–72 h on No. 1 thickness, 25-mm acid-washed glass coverslips to 20% confluency for microscopy, or on 60-mm plastic tissue culture dishes to 80% confluency for biochemical analysis.

Lipid Synthesis and Analysis

C_6-NBD-SM was synthesized from C_6-NBD-fatty acid and sphingosylphosphorylcholine by oxidation-reduction condensation with triphenylphosphine and 2-2'-dipyridyldisulfide (19, 24). TLC of the reaction mixture on silica gel 60 plates (E. Merck, Darmstadt, FRG) developed in $CHCl_3$/CH_3OH/28% NH_4OH/H_2O (72:48:2:9, vol/vol/vol/vol) resolved two products, C_6-NBD-SM1 (R_f = 0.31) and C_6-NBD-SM2 (R_f = 0.36), both having the expected molecular mass of 740.9 D as determined by mass spectrometry.

Samples of each C_6-NBD-SM isomer were hydrolyzed to C_6-NBD-ceramide (Cer) using sphingomyelinase (human placenta) in vitro as previously described (25). Reverse-phase HPLC (33) of the resulting fluorescent Cers showed that hydrolysis of C_6-NBD-SM1 produced only D-*erythro*-C_6-NBD-Cer, while hydrolysis of C_6-NBD-SM2 produced only L-*threo*-C_6-NBD-Cer. Thus, we identified C_6-NBD-SM1 as D-*erythro*-C_6-NBD-SM and C_6-NBD-SM2 as L-*threo*-C_6-NBD-SM.

N-Sulforhodamine(SRh)-conjugated dioleoylphosphatidylethanolamine (43) and *N*-(C_6-NBD)-D-*erythro*-sphingosine (C_6-NBD-Cer; 33) were synthesized and purified as previously described. Concentrations of lipid stock solutions were determined by phosphorus measurement (35) or by reference to known concentrations of fluorescent standards.

Lipid Vesicles

Small unilamellar vesicles (SUV) were formed by ethanol injection (20) as follows. C_6-NBD-SM and DOPC (typically 2:3; mol/mol) were mixed in chloroform/methanol (2:1), dried first under nitrogen, then in vacuo, and dissolved in ethanol (2.8 mM total lipid concentration). This ethanol solution was injected into 17.5 vol of 10 mM Hepes-buffered calcium and magnesium-free Puck's saline (HCMF) while vortex-mixing. The vesicle preparation was dialyzed at 4°C overnight against Hepes-buffered MEM, pH 7.4 (HMEM), and diluted to a final concentration of 25 μM total lipid in HMEM (unless otherwise specified).

DOPC vesicles for the back-exchange procedure (see below) were prepared as large unilamellar vesicles by extrusion (LUVET) as follows (14). DOPC in chloroform was dried first under nitrogen, then in vacuo, and suspended into 2 ml HCMF to obtain a final DOPC concentration of 10–40 mM. This suspension was frozen in liquid nitrogen, thawed at 37°C, frozen and thawed again, and then passed 10 times through two stacked 25-mm polycarbonate filters (0.1 μm pore size; Nuclepore Corp., Pleasanton, CA) in an extruder device (Lipex Biomembranes, Inc., Vancouver, Canada) at 250 lb/in^2. The resulting LUVETs were diluted with HMEM to a final concentration of 400 μM DOPC in HMEM.

Incubation of Lipid Vesicles with Cells

Monolayer cultures were cooled to 7°C for 5 min, washed twice with HMEM and then incubated with vesicles containing fluorescent lipid, typically using 25 μM C_6-NBD-SM/DOPC (2:3; mol/mol) SUV in HMEM at 7°C for 30 min (standard conditions). Incubations were stopped by washing the cells three times with cold HMEM. In most experiments, the cultures were subsequently warmed to 37°C by adding prewarmed HMEM to the cells and incubating at 37°C in a water-saturated incubator.

To remove C_6-NBD-SM associated with the plasma membrane, the cells were back-exchanged (37, 40) by incubating at 7°C with back-exchange medium (DOPC LUVETs in HMEM; see above). The back-exchange medium was replaced every 5 min with fresh 7°C back-exchange medium for a total of six treatments.

After back-exchange, cultures sometimes were further incubated at 37°C with either prewarmed HMEM alone or prewarmed HMEM containing back-exchange medium (to remove any C_6-NBD-lipid transported to the plasma membrane during the second 37°C incubation). After each 15-min period of reincubation at 37°C, the medium was replaced with the same type of prewarmed medium.

Analysis of Fluorescent Lipid Metabolism

Monolayer cultures of cells treated with fluorescent lipid were scraped into 1 ml HMEM with a policeman (Teflon, Wilmington, DE). The culture dish was washed with an additional 1 ml HMEM that was combined with the cell suspension. The cell suspension was centrifuged at 500 *g* for 5 min at 4°C, and the resulting cell pellet was resuspended in 200 μl HMEM. A 40-μl aliquot of this suspension was assayed for DNA content with either bisbenzimide H 33258 (21) or diphenylamine (23) using a salmon sperm DNA standard. Triton X-100 was added to the remaining 160 μl to a final concentration of 1% (wt/vol), and the NBD and SRh fluorescence was measured using a fluorimeter (model 8000C; SLM Instruments, Inc., Urbana, IL). The amounts of C_6-NBD-SM or *N*-SRh-dioleoyl phosphatidylethanolamine in HMEM present were determined by reference to standard curves.

To examine C_6-NBD-SM metabolism, the cell pellet was resuspended in 900 μl HMEM. A 100-μl aliquot of this suspension was assayed for DNA content, and the lipids were extracted from the remaining 800 μl using the procedure of Bligh and Dyer (3) using 0.9% NaCl and 10 mM HCl in the aqueous phase. Lipid extracts were chromatographed on silica gel 60 thin-layer plates using $CHCl_3$/CH_3OH/28% NH_4OH/H_2O (72:48:2:9, vol/vol/vol/vol) as the developing solvent. TLC plates were analyzed quantitatively as follows. A Newvicon camera (Dage-MTI Inc., Michigan City, IN) was used to obtain a video image of a TLC plate illuminated by UV light. The video image was then digitized using an IP-512 image processing system (Imaging Technology, Inc., Woburn, MA). Regions of the digitized image corresponding to areas of the plate containing a single C_6-NBD-lipid species were identified by the operator as regions to be quantified. Blank areas adjacent to selected regions were used to determine the amount of background signal resulting from the TLC plate. The amount of NBD fluorescence was then calculated as the difference between the total intensity within each region and the background intensity. Absolute amounts of the C_6-NBD-lipid species were determined by reference to known amounts of fluorescent lipid chromatographed and analyzed under the same conditions.

Calculation of Results

The percentage of C_6-NBD-SM removed by the back-exchange process % $(C_6\text{-NBD-SM})_{rem}$ was calculated using the equation

$$\%(C_6\text{-NBD-SM})_{rem} = [1 - ((C_6\text{-NBD-SM})_{BX}/(C_6\text{-NBD-SM})_{tot})] \times 100, \quad (1)$$

where the amount of C_6-NBD-SM was determined as pmole fluorescent SM/μg DNA in both back-exchanged cells $(C_6\text{-NBD-SM})_{BX}$ and non-back-exchanged cells $(C_6\text{-NBD-SM})_{tot}$. The amount of C_6-NBD-lipid removed by back-exchange reflects the amount of fluorescent lipid located at the plasma membrane (25, 27, 37, 44).

The amount of newly synthesized C_6-NBD-SM in D-*erythro*-C_6-NBD-SM-labeled cells was calculated from the amount of cell-associated C_6-NBD-glucosylceramide (GlcCer) by:

$$\text{(newly synthesized } C_6\text{-NBD-SM)} = 1.41 \cdot (C_6\text{-NBD-GlcCer}), \quad (2)$$

where 1.41 was the ratio of C_6-NBD-SM to C_6-NBD-GlcCer synthesized by CHO-K1 cells following incubation with D-*erythro*-C_6-NBD-Cer (see

Results). The amount of C_6-NBD-SM that was not metabolized was determined by:

$$\text{(nonmetabolized } C_6\text{-NBD-SM)} = \text{(total } C_6\text{-NBD-SM)} - \text{(newly synthesized } C_6\text{-NBD-SM)}. \quad (3)$$

Values in Eqs. 2 and 3 were determined as pmole C_6-NBD-SM/μg DNA.

Microscopy and Rh-Transferrin Labeling Procedures

A microscope (model IM-35, Carl Zeiss, Inc., Thornwood, NY) equipped with epifluorescence optics was used. Filter combinations eliminated crossover between NBD and rhodamine fluorescence channels.

Rhodamine-conjugated transferrin (Rh-Tf) was kindly provided by Drs. T. McGraw and F. Maxfield (Columbia University). For colocalization studies, cells were first labeled with C_6-NBD-SM for 30 min at 7°C, washed, and then incubated at 37°C for 30 min in HMEM containing 20 μg/ml Rh-Tf. The cells were then treated with back-exchange medium at 7°C and photographed sequentially using optics appropriate for NBD and rhodamine fluorescence.

Lysosome Labeling

Lysosomes were visualized by indirect immunofluorescence using an antibody to a 95-kD lysosomal glycoprotein (anti-lgp95), kindly provided by Drs. S. Schmid and I. Mellman (Yale University). Cells were first labeled with C_6-NBD-SM for 30 min at 7°C and then warmed for 30 min at 37°C, followed by treatment with back-exchange medium at 7°C. All remaining steps were performed at room temperature. The cells were fixed (22) using 3% paraformaldehyde-0.02% glutaraldehyde in PBS for 15 min, washed, and then photographed using optics appropriate for NBD fluorescence. The samples were then treated with 0.2 M glycine in H_2O for 5 min, followed by a 10-s treatment with 100% methanol at −20°C to render the cells permeable to antibodies. The cells were then washed with PBS containing 0.2% gelatin, and incubated with anti-lgp95 at a 1:100 dilution in PBS-gelatin for 30 min. The cells were washed, incubated with rhodamine-conjugated rabbit anti-mouse IgG at a 1:100 dilution in PBS-gelatin for 30 min, and then washed with PBS. Cells previously photographed were relocated and photographed using optics appropriate for rhodamine fluorescence.

Alternatively, cells were labeled with C_6-NBD-SM for 30 min at 7°C and then warmed to 37°C for 1 h in HMEM containing 2 mg/ml SRh-dextran (10 kD), followed by a 1-h incubation at 37°C in HMEM alone (6, 39). The cells were treated with back-exchange medium at 7°C and then photographed using optics appropriate for both NBD and rhodamine fluorescence.

Centriole Labeling

Centrioles were visualized by indirect immunofluorescence using autoantibody 5051 (4), kindly provided by Drs. T. Mitchison and M. Kirschner (University of California at San Francisco). Cells were labeled with C_6-NBD-SM for 30 min at 7°C and then warmed for 15 min at 37°C. All remaining steps were performed at room temperature. The cells were fixed using 1.6% paraformaldehyde in fixing buffer (0.1 M sodium cacodylate/0.1 M sucrose) for 15 min and photographed using optics appropriate for NBD fluorescence. The samples were then treated with 0.1% Triton X-100 in fixing buffer for 3 min, washed with HCMF, and incubated with autoantibody 5051 at a 1:100 dilution in HCMF for 30 min. The cells were washed, incubated with Rh-conjugated goat anti-human IgG at 1:200 dilution in HCMF for 30 min, and then washed with HCMF. Cells previously photographed were relocated and photographed using optics appropriate for Rh fluorescence.

Golgi Complex Labeling

Cells were labeled with 25 μM C_6-NBD-Cer/DOPC (2:3; mol/mol) SUV in HMEM at 7°C for 30 min, washed and then incubated for 30 min at 37°C in HMEM containing 5% FBS, conditions that have been previously used to label the Golgi apparatus (26). All remaining steps were performed at room temperature. The cells were fixed using 3% paraformaldehyde-0.02% glutaraldehyde in PBS for 15 min, washed, and then photographed using optics appropriate for NBD fluorescence. The samples were then treated with 0.2 M glycine in H_2O for 5 min, followed by a 10-s treatment with 100% methanol at −20°C to render the cells permeable to proteins. The cells were then washed with PBS containing 0.2% gelatin and incubated with Rh-conjugated *Ricinus communis* agglutinin 120 at 100 μg/ml in PBS-gelatin for 30 min to label the Golgi apparatus (46). The cells were washed with PBS-gelatin and cells previously photographed were relocated and photographed using optics appropriate for Rh fluorescence.

Miscellaneous Procedures

Nocodazole. Cells were preincubated with nocodazole (10 μg/ml) for 90 min at 37°C by adding a 1000× nocodazole stock solution (in DMSO) to the culture medium. All incubation solutions contained 10 μg/ml nocodazole.

Monensin. Cells were preincubated with monesin (10 μM) for 90 min at 37°C by adding a 1000× stock solution (in ethanol) into the culture medium. All incubation solutions contained 10 μM monensin.

Energy depletion was performed by incubating cells at 7°C with SUV containing fluorescent lipid in the presence of 5 mM sodium azide and 50 mM 2-deoxyglucose for 30 min, followed by 37°C incubation in HMEM containing 5 mM sodium azide and 50 mM 2-deoxyglucose for 30 min (37).

Results

C_6-NBD-SM Labeling and Internalization

The amount of spontaneous transfer of C_6-NBD-SM from SUV to CHO-K1 monolayers at 7°C was determined as a function of time, SUV concentration, or mole fraction of C_6-NBD-SM in the SUV (Fig. 1). The amount of each C_6-NBD-SM isomer incorporated into CHO-K1 cells incubated with 25 μM C_6-NBD-SM/DOPC (2:3; mol/mol) SUV in HMEM for 30 min at 7°C (standard conditions) is given in Table I. In some experiments, the SUV used for labeling also contained 2 mole % *N*-SRh-DOPE, a nonexchangeable fluorescent lipid marker (37, 40, 41) that provided a measure of SUV nonspecifically adsorbed to the cells. From these experiments, we calculate that >96% of the cell-associated C_6-NBD-SM fluorescence was the result of transfer of fluorescent SM to the plasma membrane of cells treated under standard incubation conditions.

Cells labeled with SUV containing C_6-NBD-SM at 7°C

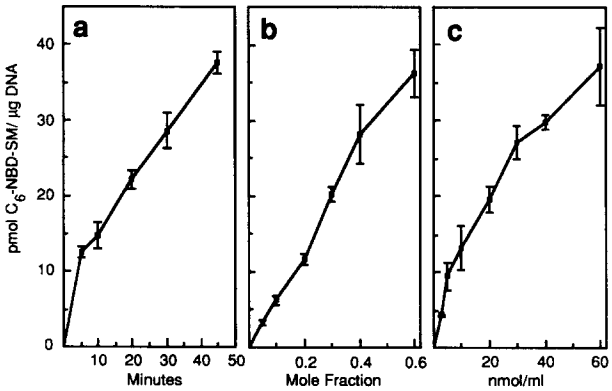

Figure 1. C_6-NBD-SM uptake by CHO-K1 cells. (*a*) Cells were incubated at 7°C with L-*threo*-C_6-NBD-SM/DOPC (2:3, mol/mol) SUV at 25 μM total lipid concentration for various times. (*b*) Cells were incubated at 7°C with SUV containing various mole fractions of L-*threo*-C_6-NBD-SM in the SUV at 25 μM total lipid concentration for 30 min. (*c*) Cells were incubated at 7°C with L-*threo*-C_6-NBD-SM/DOPC (2:3, mol/mol) SUV at various total lipid concentrations for 30 min. In each case, the cell-associated lipids were extracted, and the amount of C_6-NBD-SM was determined and normalized to total cell DNA (see Materials and Methods). Data points are the mean of triplicate measurements ± SD.

Table I. Insertion of C_6-NBD-SM into the Plasma Membrane

SM isomer	pmol/μg cell DNA	pmol/nmol cell phospholipid
D-erythro-C_6-NBD-SM	36.3 ± 6.0 (n = 6)	22.9
L-threo-C_6-NBD-SM	26.7 ± 3.0 (n = 9)	16.8

Cells were incubated with each C_6-NBD-SM isomer under standard labeling conditions, and the amount of specific incorporation of C_6-NBD-SM was measured. CHO-K1 cells contained 19.9 ± 1.5 (n = 3) μg DNA/10^6 cells and 31.6 ± 2.8 (n = 3) nmol phospholipid/10^6 cells.

showed intense plasma membrane fluorescence (Fig. 2 *a*). As long as labeled cells were kept at 7°C, at least 95.5% of the cell-associated fluorescent lipid could be removed by back-exchange. When cells labeled at 7°C were warmed to 37°C, internalization of the fluorescent lipid was observed (Fig. 2, *b–d*). With increasing time at 37°C, there was an accumulation of fluorescent lipid in intracellular vesicles, and, by 10 min, most of these vesicles had been transported to a central, perinuclear region of the cell. For 37°C incubations of 30 min or less, internalized D-*erythro* and L-*threo*-C_6-NBD-SM showed the same labeling pattern (compare Fig. 2 *d* to Fig. 3 *a*). Incubation of cells in the presence of 5 mM sodium azide and 50 mM 2-deoxyglucose inhibited endocytosis of C_6-NBD-SM from the plasma membrane (not shown), supporting the notion that C_6-NBD-SM internalization is energy-dependent.

When high concentrations of C_6-NBD-SM are incorporated into membranes, self-quenching of the probe can occur (27, 29, 37). To determine if self-quenching of C_6-NBD-SM was occurring, cells were labeled with C_6-NBD-SM at 7°C, washed, incubated at 37°C for varying amounts of time, washed, and then the amount of fluorescence in the presence or absence of 2% Triton X-100 was determined. The ratio of fluorescence in the presence or absence of Triton X-100 for C_6-NBD-SM–labeled cells that were incubated at 37°C for 0, 30, and 60 min was 1.57 ± 0.07, 1.57 ± 0.08, and 1.58 ± 0.01, respectively (n = 3 in each case), suggesting that neither the plasma membrane nor intracellular compartments contained C_6-NBD-SM at self-quenching concentrations. Also, preliminary results using low light–level digital imaging microscopy have shown that CHO-K1 cells labeled with 100-fold less C_6-NBD-SM (equivalent to 0.02% of the total

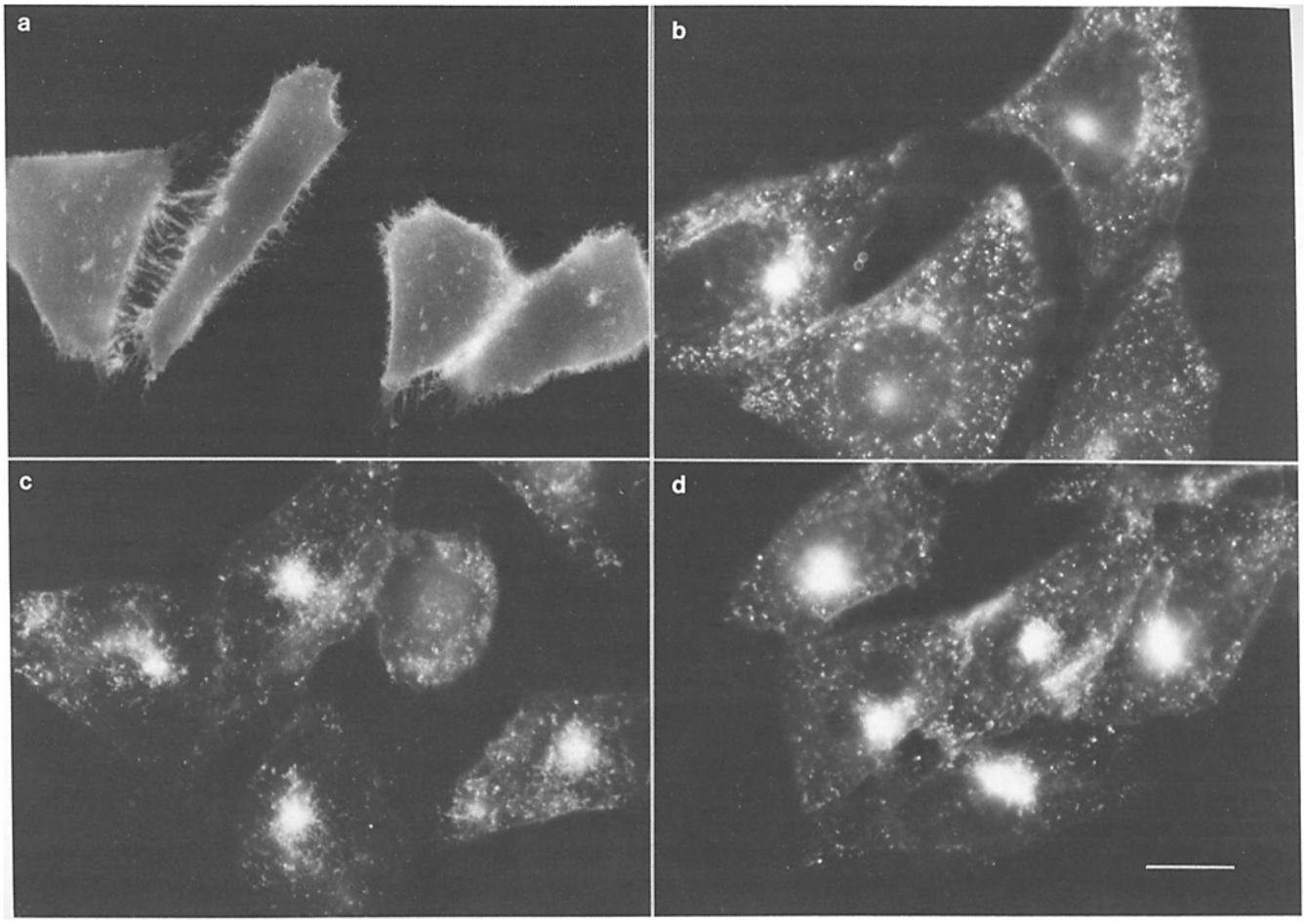

Figure 2. Appearance of C_6-NBD-SM labeling and internalization in CHO-K1 cells. (*a*) CHO-K1 cells were labeled with D-*erythro*-C_6-NBD-SM/DOPC (2:3, mole/mole) SUV at 25 μM total lipid concentration for 30 min at 7°C, washed, and photographed. Cells labeled as in *a* were washed; incubated at 37°C in HMEM for (*b*) 5 min, (*c*) 10 min, or (*d*) 30 min; treated with back-exchange medium at 7°C to remove any C_6-NBD-SM remaining at the plasma membrane; washed; and then photographed. Bar, 10 μm.

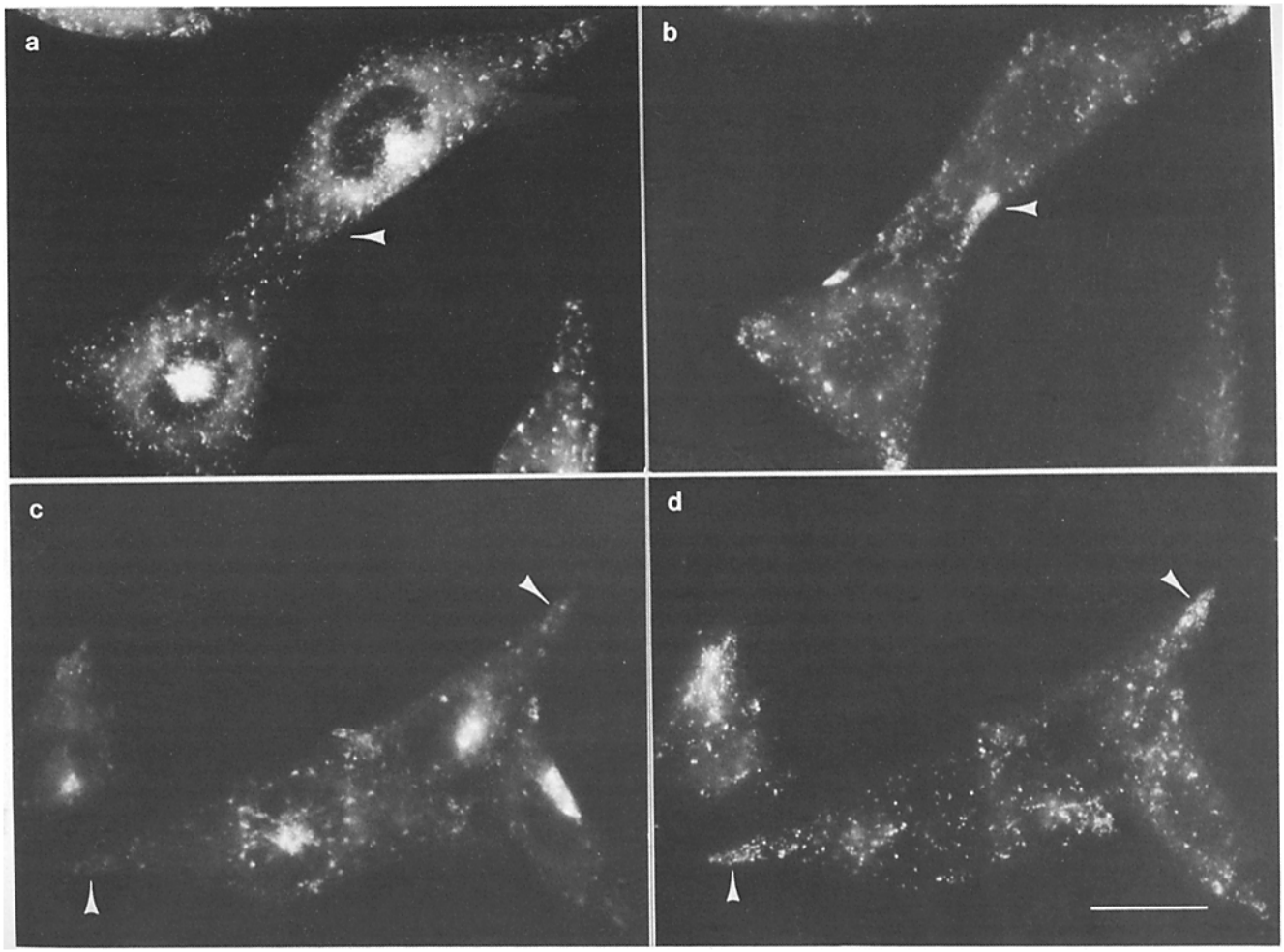

Figure 3. Comparison of endocytosed C_6-NBD-SM with lysosomal markers. (*a* and *b*) Cells were labeled with SUV containing L-*threo*-C_6-NBD-SM for 30 min at 7°C, washed, and incubated in HMEM for 30 min at 37°C. The cells were then treated with back-exchange medium at 7°C to remove any C_6-NBD-SM remaining at the plasma membrane, washed, fixed and photographed for C_6-NBD-lipid fluorescence (*a*). The cells were subsequently rendered permeable, treated with an antilysosomal antibody (anti-lgp95), and then labeled with Rh-conjugated rabbit anti-mouse IgG. The cells were washed and the field previously photographed for C_6-NBD-lipid fluorescence was rephotographed for Rh fluorescence (*b*). (*c* and *d*) Cells were labeled with SUV containing D-*erythro*-C_6-NBD-SM in HMEM for 30 min at 7°C, washed, and incubated for 1 h at 37°C in HMEM containing 2 mg/ml SRh-dextran. The cells were then washed and further incubated for 1 h at 37°C in HMEM alone, treated with back-exchange medium at 7°C to remove C_6-NBD-SM remaining at the plasma membrane, washed, and photographed for either (*c*) C_6-NBD-lipid or (*d*) SRh-dextran fluorescence. This procedure does not require relocation of labeled cells and thus minimizes the possibility of a change in the plane of focus during photography. Note the absence of NBD and SRh fluorescence colocalization (*arrowheads*). Bar, 10 μm.

cell phospholipid) endocytose fluorescent SM to the perinuclear region of the cell (not shown), suggesting that the addition of larger amounts of C_6-NBD-SM to the plasma membrane was not affecting the internalization process.

Characterization of Compartments Labeled by Endocytosed C_6-NBD-SM

To determine whether internalized C_6-NBD-SM was transported to the lysosomes, cells were first labeled with fluorescent SM under standard conditions and incubated for 30 min at 37°C, followed by back-exchange. The cells were then subsequently labeled with anti-lgp95, which recognizes a 95-kD lysosomal glycoprotein (Fig. 3, *a* and *b*). Note the lack of lysosomes in the central region of the cell, in contrast to the intracellular vesicles labeled by internalized C_6-NBD-lipid. Also, it appeared that very little fluorescent lipid accumulated in the lysosomes under these conditions as indicated by a lack of probe colocalization. In a complementary experiment (Fig. 3, *c* and *d*), cells were labeled with C_6-NBD-SM under standard conditions and then incubated at 37°C for 1 h in the presence of the fluid phase marker SRh-dextran, followed by a 1-h chase at 37°C in HMEM alone to insure that the SRh-dextran was transported to the lysosomes (39). Even after a 2-h incubation at 37°C, little, if any, C_6-NBD-lipid appeared to have accumulated in the lysosomes.

Cells containing internalized C_6-NBD-SM were also subsequently labeled with an antibody that labels pericentriolar material (4). Endocytic vesicles containing fluorescent lipid aggregated around the centriole in C_6-NBD-SM–labeled CHO-K1 cells (Fig. 4, *a* and *b*). Since the centriole acts as

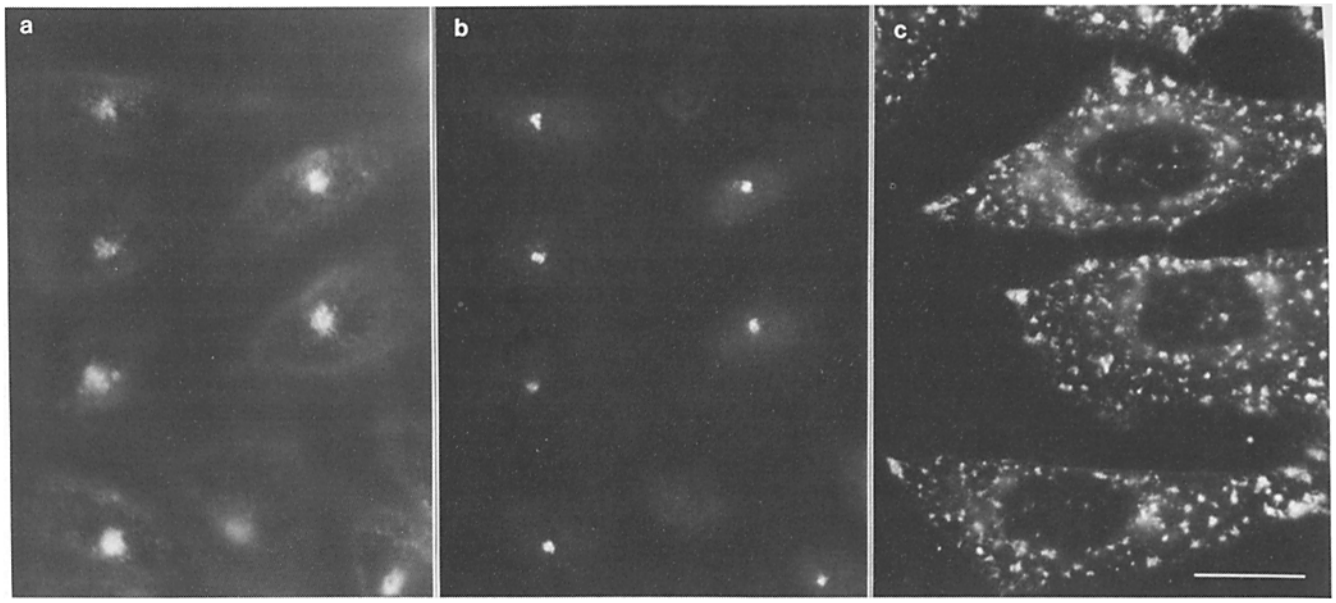

Figure 4. Colocalization of endocytosed C_6-NBD-SM with the centriole and the effect of microtubule disruption on C_6-NBD-SM internalization. In (*a* and *b*), cells were labeled with SUV containing L-*threo*-C_6-NBD-SM for 30 min at 7°C, washed, and incubated in HMEM for 15 min at 37°C. The cells were then treated with back-exchange medium at 7°C to remove any C_6-NBD-SM remaining at the plasma membrane, washed, fixed and photographed for C_6-NBD-lipid fluorescence (*a*). Note that the plane of focus selected does not enable the visualization of fluorescently labeled peripheral endosomes. The cells were subsequently rendered permeable, treated with antibody 5051, which recognizes pericentriolar material, and then labeled with Rh-conjugated goat anti-human IgG. The cells were washed and the field previously photographed for C_6-NBD-lipid fluorescence was rephotographed for Rh fluorescence (*b*). (*c*) Cells were preincubated with 10 μg/ml nocodazole for 90 min at 37°C in culture medium, washed, and labeled with SUV containing L-*threo*-C_6-NBD-SM in HMEM with 10 μg/ml nocodazole. The cells were washed, incubated with back-exchange medium containing 10 μg/ml nocodazole at 7°C to remove any C_6-NBD-SM remaining at the plasma membrane, washed, and photographed. Bar, 10 μm.

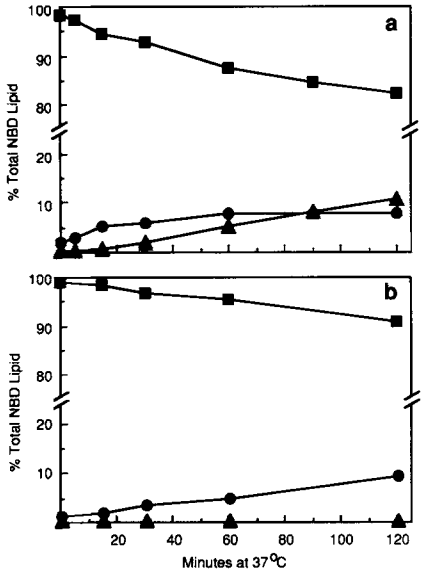

Figure 5. Metabolism of D-*erythro* and L-*threo*-C_6-NBD-SM. Cells were labeled with SUV containing either (*a*) D-*erythro*- or (*b*) L-*threo*-C_6-NBD-SM in HMEM for 30 min at 7°C, washed and incubated for the indicated times at 37°C in HMEM. The cell-associated lipids were extracted, separated by TLC, and the fluorescent metabolites were measured and expressed as a percentage of total cell-associated C_6-NBD-lipid. (■) C_6-NBD-SM; (▲) C_6-NBD-GlcCer; (●) C_6-NBD-Cer. Data points are the mean of triplicate measurements.

a microtubule organizing center, the effect of microtubule disruption was also examined. In the presence of 10 μg/ml nocodazole, C_6-NBD-SM continued to be endocytosed, however, microtubule disruption resulted in little internalized fluorescent lipid accumulation in the central region of the cells. Instead, C_6-NBD-lipid was distributed in vesicles throughout the periphery of the cell (Fig. 4c).

Quantitation of Metabolism and Endocytosis of C_6-NBD-SM

Cells labeled with either D-*erythro* or L-*threo*-C_6-NBD-SM at 7°C under standard conditions and then incubated at 37°C metabolized C_6-NBD-SM to other fluorescent sphingolipids (Fig. 5, *a* and *b*). Both C_6-NBD-SM isomers showed partial hydrolysis to the corresponding C_6-NBD-Cer isomer, but only D-*erythro*-C_6-NBD-SM–labeled cells produced C_6-NBD-GlcCer (from C_6-NBD-Cer) during the 37°C incubation, probably because of the stereospecificity of the conversion of C_6-NBD-Cer to C_6-NBD-GlcCer (33). No other fluorescent lipid species, including C_6-NBD-fatty acid, were produced during 37°C incubations of up to 6 h in cells labeled with either fluorescent SM isomer. In addition, a small amount (1.7 ± 0.7%; n = 3) of D-*erythro*-C_6-NBD-SM was hydrolyzed to C_6-NBD-Cer during the 30 min incubation at 7°C.

CHO-K1 cells were labeled directly with D-*erythro*-C_6-NBD-Cer and the conversion to C_6-NBD-SM and C_6-NBD-

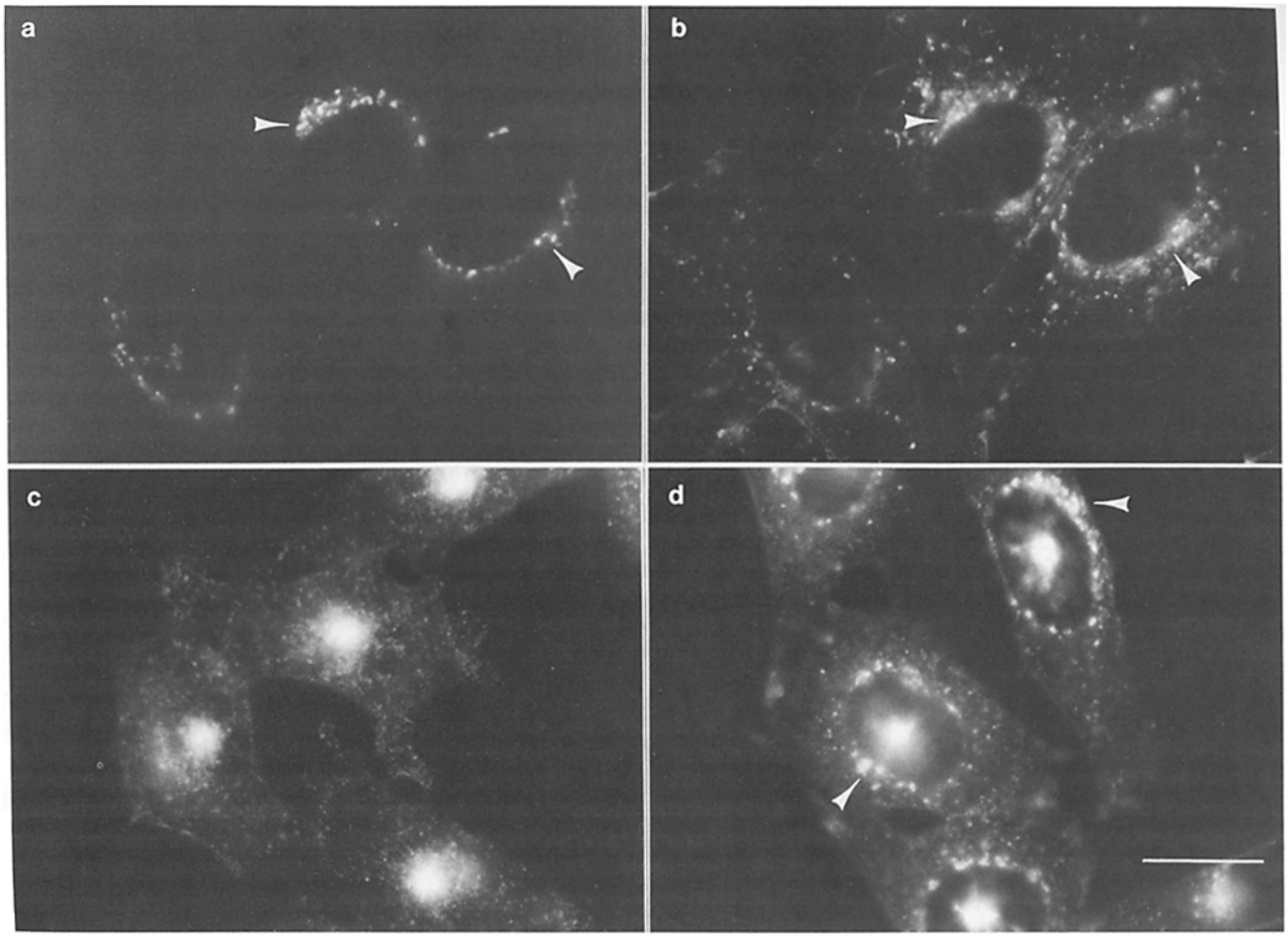

Figure 6. C_6-NBD-Cer labeling of the Golgi apparatus. (*a* and *b*) CHO-K1 cells were labeled with SUV containing D-*erythro*-C_6-NBD-Cer in HMEM for 30 min at 7°C, washed, incubated for 30 min at 37°C in HMEM containing 5% FBS, fixed, and then photographed for C_6-NBD-lipid fluorescence (*a*). The cells were then rendered permeable, and treated with Rh-conjugated *Ricinus communis* agglutinin 120, which preferentially labels the Golgi apparatus (34, 46). The cells were washed, and the field, previously photographed for C_6-NBD-lipid fluorescence, was rephotographed for Rh fluorescence (*b*). Note labeling around the perimeter of the nucleus (*arrowheads*). (*c* and *d*) Cells were labeled with SUV containing D-*erythro*-C_6-NBD-SM at 7°C, washed, incubated for 30 min (*c*) or 2 h (*d*) at 37°C in HMEM, followed by treatment with back-exchange medium at 7°C and then photographed. Note the appearance of fluorescence around the perimeter of the nucleus with increasing time at 37°C (*arrowheads*) in addition to labeling of the central perinuclear region. Bar, 10 μm.

GlcCer during 37°C incubation was examined under a wide range of conditions. Cells were labeled at 7°C for 30 min with C_6-NBD-Cer/DOPC (2:3, mol/mol) SUV (*a*) at concentrations ranging from 3 to 50 μM total lipid, washed, and then incubated for 30 min at 37°C, or (*b*) at 25 μM total lipid, washed, and then incubated at 37°C for times ranging from 5 min to 2 h. In all cases both C_6-NBD-SM and C_6-NBD-GlcCer were synthesized from fluorescent Cer. The ratio (C_6-NBD-SM produced/C_6-NBD-GlcCer produced) was 1.41 ± 0.33 (n = 26). D-*erythro*-C_6-NBD-Cer metabolism was not affected when cells were treated with either 10 μg/ml nocodazole or 10 μM monensin.

The intracellular distribution of exogenously supplied D-*erythro*-C_6-NBD-Cer was examined in CHO-K1 cells. Cells labeled with SUV containing fluorescent Cer at 7°C for 30 min followed by 37°C incubation for 30 min showed prominent labeling largely around the perimeter of the nucleus (Fig. 6 *a*). To confirm that C_6-NBD-Cer labeled the Golgi apparatus in CHO cells, as previously shown in other cell types (26), the intracellular distributions of C_6-NBD-Cer and a lectin that preferentially labels the Golgi apparatus (Rh-*Ricinus communis* agglutinin 120; 34, 46) were compared. As seen in Fig. 6 (*a* and *b*) Rh-RCA and C_6-NBD-Cer fluorescence extensively colocalized, although subtle differences, possibly because of a slight change in the plane of focus, were observed. In contrast, cells labeled with C_6-NBD-SM under standard conditions and then incubated at 37°C for 30 min largely contained intracellular fluorescent lipid in a central, perinuclear region of the cell with little labeling around the perimeter of the nucleus (Fig. 6 *c*). However, with increasing incubation time at 37°C, C_6-NBD-SM–labeled cells showed increasing amounts of labeling around the perimeter of the nucleus in addition to labeling of the central perinuclear region (Fig. 6 *d*). These data suggest that, during 37°C incubations of fluorescent SM-labeled cells, C_6-NBD-Cer produced by the hydrolysis of C_6-NBD-SM was transported to the Golgi apparatus.

To determine whether some of the cell-associated C_6-

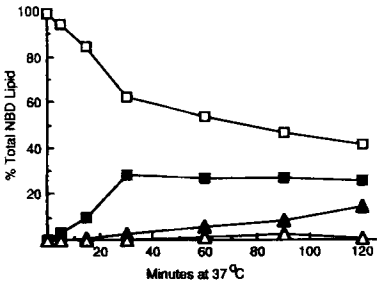

Figure 7. Quantitative distribution of C_6-NBD-SM upon 37°C incubation. CHO-K1 cells were labeled with SUV containing D-*erythro*-C_6-NBD-SM in HMEM for 30 min at 7°C, washed, incubated at 37°C in HMEM for the indicated amount of time, and then either harvested immediately or, in parallel experiments, after treatment with back-exchange medium at 7°C to remove any C_6-NBD-lipid at the plasma membrane. The cell-associated lipids were extracted and analyzed by TLC as described in the text. The amount of back-exchangeable C_6-NBD-lipid was calculated using Eq. 1 (see Materials and Methods) and all values are expressed as percentage of total cell-associated C_6-NBD-lipid. The amounts of newly synthesized C_6-NBD-SM and nonmetabolized C_6-NBD-SM were calculated by Eq. 2 and 3, respectively (see Materials and Methods). (□) Nonmetabolized D-*erythro*-C_6-NBD-SM at the plasma membrane; (■) intracellular nonmetabolized D-*erythro*-C_6-NBD-SM; (△) newly synthesized D-*erythro*-C_6-NBD-SM at the plasma membrane; (▲) intracellular newly synthesized D-*erythro*-C_6-NBD-SM. Data points are the mean of triplicate measurements.

NBD-SM resulted from the hydrolysis of fluorescent SM to C_6-NBD-Cer followed by resynthesis of C_6-NBD-SM, cells were prelabeled with [^{32}P]orthophosphate followed by incubation with SUV containing either D-*erythro* or L-*threo*-C_6-NBD-SM at 7°C. The cells were then washed, incubated at 37°C for 2 h, and the cell-associated lipids were extracted and analyzed by two-dimensional TLC. In both cases, C_6-NBD-SM isolated from these cells had incorporated ^{32}P (not shown), suggesting that two pools of fluorescent SM were present; i.e., nonmetabolized and newly synthesized C_6-NBD-SM.

The best resolution of C_6-NBD-SM from other radiolabeled lipids possible by TLC was adequate for autoradiography, but not for quantitative determination of ^{32}P incorporation. Because CHO-K1 cells directly labeled with D-*erythro*-C_6-NBD-Cer produced C_6-NBD-SM and C_6-NBD-GlcCer at a constant ratio (1.41:1), we used the amount of cell-associated fluorescent GlcGer to estimate the amount of newly synthesized C_6-NBD-SM formed by D-*erythro*-C_6-NBD-SM-labeled cells during a given experiment (Eq. 2). The amount of nonmetabolized C_6-NBD-SM was then calculated as the difference between the total cell-associated C_6-NBD-SM and the amount of newly synthesized C_6-NBD-SM (Eq. 3). L-*threo*-C_6-NBD-SM-labeled cells did not produce any C_6-NBD-GlcCer; therefore, all quantitation of C_6-NBD-SM transport was done using D-*erythro*-C_6-NBD-SM-labeled cells.

Fig. 7 shows the quantitative redistribution of fluorescent SM in D-*erythro*-C_6-NBD-SM-labeled CHO-K1 cells during a 37°C incubation. C_6-NBD-SM levels at the plasma membrane declined as the result of fluorescent SM endocytosis and hydrolysis to C_6-NBD-Cer. The amount of endocytosed, nonmetabolized C_6-NBD-SM reached a plateau value of ~27% of the total cell-associated C_6-NBD-lipid after 30 min at 37°C. The amount of newly synthesized C_6-NBD-SM produced during the 2-h incubation period increased steadily to ~15% of the total C_6-NBD-lipid, but remained less than the amount of internalized, nonmetabolized C_6-NBD-SM. Also, only small amounts of newly synthesized fluorescent SM were transported to the plasma membrane during this period (~3% of the total C_6-NBD-lipid). Neither 10 μM monensin nor 10 μg/ml nocodazole inhibited either the C_6-NBD-SM internalization or C_6-NBD-GlcCer synthesis in C_6-NBD-SM-labeled cells (Table II).

Plasma Membrane Recycling of C_6-NBD-SM

Cells were labeled with C_6-NBD-SM under standard conditions, washed, incubated at 37°C for 30 min and then treated with back-exchange medium at 7°C to remove any fluorescent SM remaining at the plasma membrane, resulting in cells containing only internalized fluorescent lipid (Fig. 8 *a*). Cells containing only internalized fluorescent lipid were further incubated at 37°C in HMEM and the transport of C_6-NBD-lipid from intracellular compartments to the plasma membrane was observed (Fig. 8 *b*). When cells that had been further incubated at 37°C were subsequently treated with back-exchange medium at 7°C, to remove any fluorescent lipid that had returned to the plasma membrane, C_6-NBD-lipid labeling in the periphery of the cell was revealed (Fig. 8 *c*). In contrast, when cells containing only internalized C_6-NBD-lipid were further incubated at 37°C in back-exchange medium, any C_6-NBD-lipid transported to the plasma membrane from intracellular compartments was contin-

Table II. Effect of Nocodazole and Monensin on C_6-NBD-SM Endocytosis

	C_6-NBD-SM internalized		C_6-NBD-GlcCer synthesized	
Treatment	pmol/μg DNA	Percent of cell-associated C_6-NBD-lipid	pmol/μg DNA	Percent of cell-associated C_6-NBD-lipid
Control	5.24 ± 0.60	28.1 ± 3.2	0.33 ± 0.05	1.7 ± 0.3
10 μM monensin	6.20 ± 2.10	33.3 ± 11.3	0.53 ± 0.11	2.8 ± 0.6
10 μg/ml nocodazole	3.76 ± 0.39	37.9 ± 3.9	0.40 ± 0.04	4.0 ± 0.4

Cells were either untreated (control) or were preincubated with 10 μM monensin or 10 μg/ml nocodazole in culture medium for 90 min at 37°C. All solutions used for treated cells contained either 10 μM monensin or 10 μg/ml nocodazole. Cells were labeled with SUV containing D-*erythro*-C_6-NBD-SM in HMEM for 30 min at 7°C, washed, incubated in HMEM at 37°C for 30 min, and either harvested immediately or treated with back-exchange medium at 7°C. The cell-associated lipids were extracted, and both the amount of endocytosed, nonmetabolized C_6-NBD-SM and of newly synthesized C_6-NBD-GlcCer were determined as described in the legend to Fig. 7. Data are the mean of triplicate measurements ± SD.

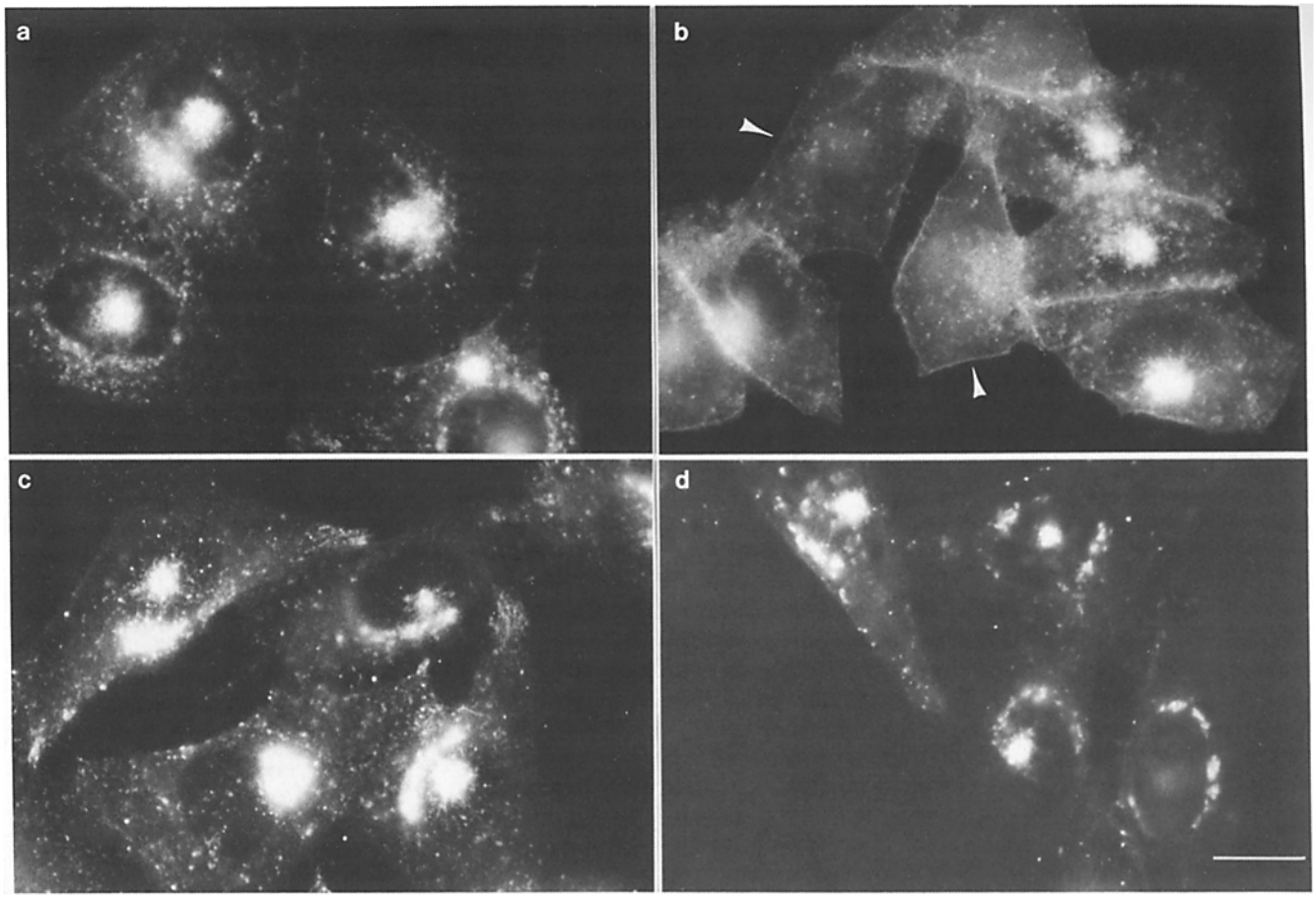

Figure 8. Recycling of intracellular C_6-NBD-SM to the plasma membrane. (*a*) Cells were labeled with SUV containing D-*erythro*-C_6-NBD-SM in HMEM for 30 min at 7°C, washed, incubated at 37°C for 30 min in HMEM, and treated with back-exchange medium at 7°C resulting in cells containing only internalized C_6-NBD-lipid. (*b*) Cells treated as in *a* were further incubated at 37°C in HMEM for 30 min, washed, and photographed. The plasma membrane (*arrowheads*) showed the reappearance of fluorescent lipid labeling. (*c*) Cells treated as in *b* were then treated with back-exchange medium at 7°C to remove any C_6-NBD-lipid returned to the plasma membrane, washed, and photographed. Note peripheral endosomes containing reinternalized fluorescent lipid. (*d*) Cells treated as in *a* were further incubated for 30 min at 37°C in back-exchange medium that continuously removed any C_6-NBD-lipid being transported to the plasma membrane from intracellular compartments during the 37°C incubation. The cells were then washed and photographed. Note the lack of fluorescently labeled peripheral vesicles in *d* versus *c*. In some cases, perinuclear labeling was not visible for each cell in the field because of the plane of focus selected. Bar, 10 μm.

uously removed to acceptor vesicles (Fig. 8 *d*). Cells treated in this manner showed very little labeling of intracellular vesicles in the periphery of the cell, suggesting that labeling of the cell periphery shown in Fig. 8 *c* was because of the further internalization of C_6-NBD-lipid that had been returned to the plasma membrane.

Quantitative analysis of cells containing only internalized D-*erythro*-C_6-NBD-SM that were further incubated for 30 min determined that 3.03 ± 0.22 ($n = 3$) pmole of nonmetabolized C_6-NBD-SM/μg DNA was recycled back to the plasma membrane, while the combined amount of newly synthesized C_6-NBD-SM and C_6-NBD-GlcCer resulted in only 0.46 ± 0.31 ($n = 3$) pmole/μg DNA. Thus, >86% of the plasma membrane fluorescence observed in Fig. 8 *b* was the result of the recycling of nonmetabolized C_6-NBD-SM.

The time course of nonmetabolized D-*erythro*-C_6-NBD-SM return to the plasma membrane from intracellular compartments was also determined (Fig. 9). C_6-NBD-SM was transported to the plasma membrane from intracellular compartments with a half-time of ~15–20 min. Combined with a half-time of ~15–20 min for C_6-NBD-SM internalization (Fig. 7), this gives a half-time for one complete round of recycling of ~30–40 min.

The effects of 10 μg/ml monensin on C_6-NBD-SM recycling were also examined (Table III). Similar amounts of transport of nonmetabolized, intracellular C_6-NBD-SM to the plasma membrane occurred in monensin-treated and control cells. However, transport of newly synthesized C_6-NBD-SM to the plasma membrane was abolished, consistent with previous results (25).

In spite of the altered pattern of C_6-NBD-SM internalization (Fig. 4 *c*), nocodazole-treated cells exhibited plasma membrane recycling of nonmetabolized C_6-NBD-SM (Table III). Neither the return of nonmetabolized C_6-NBD-SM to the plasma membrane nor the transport of newly synthesized C_6-NBD-SM were inhibited by nocodazole. In fact, nocodazole appeared to increase the amount of newly synthesized C_6-NBD-SM transport to the plasma membrane.

Since C_6-NBD-SM was capable of recycling, we wanted to compare the distribution of internalized C_6-NBD-SM

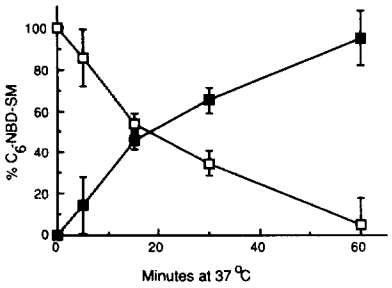

Figure 9. Quantitation of internalized C_6-NBD-SM returned to the plasma membrane. Cells were labeled with SUV containing D-*erythro*-C_6-NBD-SM in HMEM at 7°C for 30 min, washed, incubated at 37°C for 30 min, and treated with back-exchange medium at 7°C to remove any C_6-NBD-SM remaining at the plasma membrane. The cells were then further incubated for the indicated amount of time at 37°C in either HMEM or back-exchange medium, washed, and the cell-associated lipids were extracted and analyzed by TLC (see Materials and Methods). The amount of nonmetabolized C_6-NBD-SM returned to the plasma membrane was calculated using Eqs. 1-3. (■) D-*erythro*-C_6-NBD-SM and returned to the plasma membrane; (□) intracellular D-*erythro*-C_6-NBD-SM. Data points are the mean of triplicate measurements ± SD and are expressed as the percentage of total cell-associated, nonmetabolized C_6-NBD-SM.

with that of Rh-Tf, a recycling protein (45). Cells were labeled with C_6-NBD-SM at 7°C under standard conditions, washed, and then incubated for 30 min at 37°C in HMEM containing Rh-Tf. As shown in Fig. 10, both C_6-NBD-SM and Rh-Tf were internalized to the central region of the cell; however, some intracellular vesicles in the periphery of the cell appeared to be labeled only by C_6-NBD-SM. This could be, in part, because of a difference in the sensitivity of C_6-NBD-lipid detection versus Rh-Tf detection.

Discussion

In this study, we have examined the transport of the D-*erythro* and L-*threo* stereoisomers of a fluorescent analogue of sphingomyelin, C_6-NBD-SM, as probes for plasma membrane lipid transport in CHO-K1 cells. Most of the intracellular C_6-NBD-SM was transported along the recycling pathway illustrated in Fig. 11, pathway *I*. Both isomers of C_6-NBD-SM labeled only the plasma membrane when incubated with cells at 7°C. Cells labeled with C_6-NBD-SM at 7°C and then incubated at 37°C endocytosed fluorescent SM to a perinuclear region of the cell that colocalized with the centriole. When cells containing only internalized C_6-NBD-lipid were further incubated at 37°C, C_6-NBD-SM was returned to the plasma membrane. Thus, C_6-NBD-SM recycles between the plasma membrane and intracellular compartments. Both D-*erythro* and L-*threo*-C_6-NBD-SM were capable of being recycled.

In addition to the endocytosis of C_6-NBD-SM, some hydrolyis of both C_6-NBD-SM isomers to the corresponding C_6-NBD-Cer isomer was observed upon 37°C incubation. C_6-NBD-Cer can spontaneously undergo transbilayer movement (31), in contrast to C_6-NBD-SM which has a highly polar head group restricting it to one leaflet of a bilayer (17). Thus, as illustrated in Fig. 11, pathway *II*, C_6-NBD-Cer produced by the hydrolysis of C_6-NBD-SM was transported to the Golgi apparatus, presumably by spontaneous diffusion (30, 33), where it was converted back to fluorescent SM and, in the case of D-*erythro*-C_6-NBD-SM, to fluorescent GlcCer. Consistent with the synthesis of C_6-NBD-SM at the Golgi apparatus (30) and the transport of newly synthesized C_6-NBD-SM through the Golgi apparatus (25), the transport of newly synthesized C_6-NBD-SM to the plasma membrane was inhibited by monensin, while the recycling of nonmetabolized C_6-NBD-SM was not affected by monesin treatment (Table III).

Fig. 11 depicts the partial hydrolysis of C_6-NBD-SM occurring at the plasma membrane. This is consistent with our observation that some hydrolysis of D-*erythro*-C_6-NBD-SM occurred at 7°C, in the absence of endocytosis. Neutral sphingomyelinases have been found in plasma membrane-enriched fractions from rat liver (16), neuroblastoma cell cultures (5), and human renal proximal tubule cell cultures (9). It is possible that C_6-NBD-SM was also hydrolyzed by lysosomal (acid) sphingomyelinase (1, 7, 18); however, C_6-NBD-SM did not accumulate in the lysosomes, probably because of the sorting of endocytosed C_6-NBD-SM from the degradation pathway to a recycling pathway. Also, increasing lysosomal pH with NH_4Cl, which should reduce lysosomal sphingomyelinase activity, did not inhibit C_6-NBD-SM hydrolysis (data not shown). Examination of C_6-NBD-SM transport in Niemann-Pick fibroblasts, which are

Table III. Effect of Nocodazole and Monensin on C_6-NBD-SM Recycling

Treatment	Percent of total C_6-NBD-SM			
	Nonmetabolized C_6-NBD-SM recycled	New C_6-NBD-SM transported	Percent nonmetabolized C_6-NBD-SM recycled	Percent new C_6-NBD-SM transported
Control	43.3 ± 4.2	4.0 ± 2.8	68.7 ± 9.8	10.8 ± 1.0
10 μM monensin	56.1 ± 19.1	0*	76.0 ± 25.9	0*
10 μg/ml nocodazole	46.8 ± 5.9	9.9 ± 1.8	60.8 ± 7.7	43.0 ± 7.8

Cells were either untreated (control) or preincubated with 10 μM monensin or 10 μg/ml nocodazole in culture medium for 90 min at 37°C. All solutions used for treated cells contained either 10 μM monensin or 10 μg/ml nocodazole. Cells were labeled with SUV containing D-*erythro*-C_6-NBD-SM in HMEM for 30 min at 7°C, washed, incubated at 37°C in HMEM for 30 min, and then treated with back-exchange medium to remove any C_6-NBD-SM remaining at the plasma membrane. The cells were then further incubated at 37°C for 30 min in either HMEM or back-exchange medium and washed. The cell-associated lipids were extracted and both the amount of nonmetabolized C_6-NBD-SM recycled to the plasma membrane and of newly synthesized C_6-NBD-SM transported to the plasma membrane were determined as described in the legend to Fig. 9. Data are the mean of triplicate measurements ± SD, expressed as percent total cell-associated C_6-NBD-SM.

* Not detectable.

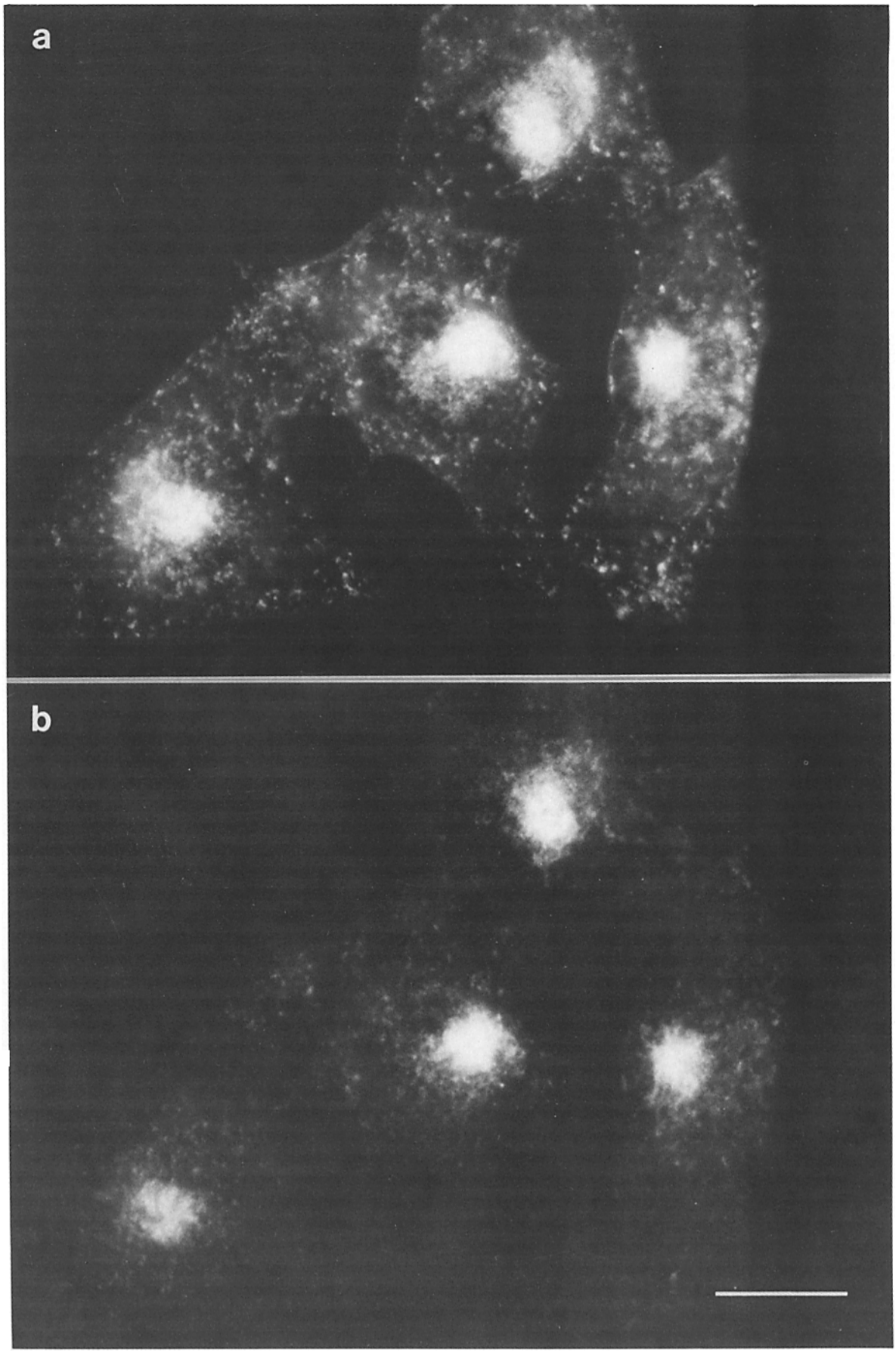

Figure 10. Colocalization of internalized C_6-NBD-SM and Rh-Tf. Cells were labeled with SUV containing D-*erythro*-C_6-NBD-SM at 7°C, washed, and incubated at 37°C for 30 min in HMEM that contained 20 μg/ml Rh-Tf. The cells were treated with back-exchange medium at 7°C to remove any C_6-NBD-SM remaining at the plasma membrane and then photographed for either C_6-NBD-lipid (*a*) or Rh-Tf (*b*) fluorescence. Bar, 10 μm.

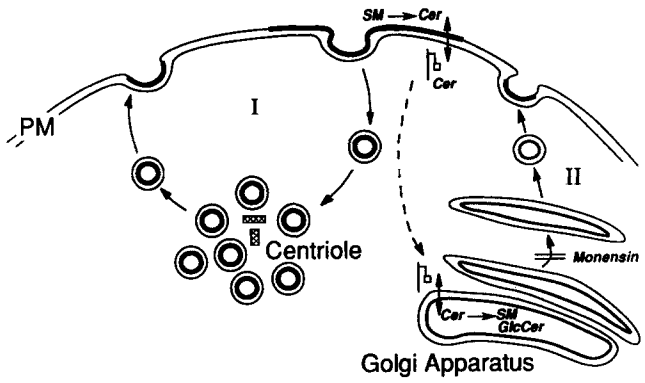

Figure II. Model of C_6-NBD-SM transport and recycling. Thick lines represent portions of the bilayer containing fluorescent lipid. Pathway *I*, nonmetabolized C_6-NBD-SM inserted into the outer leaflet of the plasma membrane (*PM*) is endocytosed to intracellular vesicles in the region of the centriole. The internalized C_6-NBD-SM is subsequently transported from intracellular compartments back to the plasma membrane, resulting in a plasma membrane lipid recycling pathway. Pathway *II*, a small amount of C_6-NBD-SM is hydrolyzed to C_6-NBD-Cer at the plasma membrane. The fluorescent Cer produced spontaneously moves to the Golgi apparatus where it is metabolized to newly synthesized C_6-NBD-SM and, in the case of D-*erythro*-C_6-NBD-Cer, to C_6-NBD-GlcCer. The metabolites are then transported from the Golgi apparatus to the plasma membrane by a process that is inhibited by monensin treatment.

deficient in lysosomal sphingomyelinase, may help determine the relative importance of these two sites of SM hydrolysis in the cell.

C_6-NBD-SM–labeled CHO-K1 cells internalized fluorescent SM that accumulated in intracellular vesicles associated with the centriole. These "perinuclear" endosomes have been observed in a variety of systems (for review, see 15) and are distinct from peripheral endosomal compartments. The Golgi apparatus is often associated with the centriole, particularly when migrating fibroblasts are examined (36). Previous work from our laboratory indicates that a fluorescent analogue of phosphatidylcholine is internalized from the plasma membrane and transported to the region of the Golgi apparatus in Chinese hamster V79 fibroblasts (37). In CHO-K1 cells, we found that the Golgi apparatus and perinuclear endosomes were not usually juxtaposed, suggesting that the extent of colocalization of these compartments depends on the cell type.

The association of intracellular compartments with microtubules has been examined elsewhere (8, 13, 28, 42). Disruption of the microtubules did not inhibit the endocytosis or recycling of C_6-NBD-SM; however, intracellular vesicles containing fluorescent SM no longer accumulated in the central region of the cell. Consistent with these results, transferrin also recycles in microtubule-disrupted cells (12). Consistent with these studies, recycling of C_6-NBD-SM was not inhibited by disruption of microtubules with nocodazole.

One round of C_6-NBD-SM recycling occurs with a half-time of ~40 min in CHO-K1 cells. In contrast, the half-time for transferrin recycling in CHO cells is ~15 min (47). The slower rate of C_6-NBD-SM recycling is not surprising, since rapidly recycling receptors are actively clustered into coated pits (10), while lipids are likely to undergo rapid random lateral diffusion throughout the plasma membrane bilayer.

Maxfield and co-workers have shown that fluorescently labeled transferrin segregates into a perinuclear compartment upon endocytosis in CHO-WTT2 cells that they identify as a postsegregation compartment along the exocytic portion of the plasma membrane recycling pathway (47). We have found that Rh-Tf and C_6-NBD-SM are endocytosed to the same compartment by CHO-K1 cells during 37°C incubation. Whether all plasma membrane proteins and lipids recycle through this compartment is unknown at present. The use of C_6-NBD-SM in conjunction with fluorescently labeled proteins will enable the simultaneous visualization and measurement of lipid and protein transport in future studies. This approach could determine the extent to which plasma membrane recycling pathways taken by proteins and lipids coincide.

We are grateful to Drs. M. Kirschner, I. Mellman, T. Mitchison, and S. Schmid for their gifts of antibodies, and to Drs. T. McGraw and F. Maxfield for providing Rh-Tf. Mass spectral determinations were carried out at the Middle Atlantic Mass Spectrometry Laboratory (Baltimore, MD). We thank Dr. J. Gall for helpful suggestions and Ms. O. Martin, Mr. A. Ting, Dr. A. Futerman, Dr. T. Kobayashi, and Dr. A. Winiski for critical reading of the manuscript.

This work was supported by United States Public Health Service grant GM-22942.

Received for publication 28 September 1988 and in revised form 16 February 1989.

References

1. Barenholz, Y., and S. Gatt. 1982. Sphingomyelin: metabolism, chemical synthesis, chemical and physical properties. *In* Phospholipids. J. N. Hawthorne and G. B. Ansell, editors. Elsevier Science Publishing Co. Inc., Amsterdam. 129–178.
2. Barenholz, Y., A. Roitman, and S. Gatt. 1966. Enzymatic hydrolysis of sphingolipids. II. Hydrolysis of sphingomyelin by an enzyme from rat brain. *J. Biol. Chem.* 241:3731–3737.
3. Bligh, E. G., and W. J. Dyer. 1959. A rapid method of total lipid extraction and purification. *Can. J. Biochem. Physiol.* 37:911–917.
4. Calarco-Gilliam, P. D., M. C. Siebert, R. Hubble, T. Mitchison, and M. Kirschner. 1983. Centrosome development in early mouse embryos as defined by an autoantibody against pericentriolar material. *Cell.* 35: 621–629.
5. Das, D. V. M., H. W. Cook, and M. W. Spence. 1984. Evidence that neutral sphingomyelinase of cultured murine neuroblastoma cells is oriented externally on the plasma membrane. *Biochim. Biophys. Acta.* 777:339–342.
6. Ferris, A. L., J. C. Brown, R. D. Park, and B. Storrie. 1987. Chinese hamster ovary cell lysosomes rapidly exchange contents. *J. Cell Biol.* 105: 2703–2712.
7. Fowler, S. 1969. Lysosomal localization of sphingomyelinase in rat liver. *Biochim. Biophys. Acta.* 191:481–484.
8. Freed, J. J., and M. M. Lebowitz. 1970. The association of a class of saltatory movements with microtubules in cultured cells. *J. Cell Biol.* 45:334–354.
9. Ghosh, P., and S. Chatterjee. 1987. Effects of gentamycin on sphingomyelinase activity in cultured human renal proximal tubular cells. *J. Biol. Chem.* 262:12550–12556.
10. Goldstein, J. L., M. S. Brown, R. G. W. Anderson, D. W. Russell, and W. J. Schneider. 1985. Receptor-mediated endocytosis: concepts emerging from the LDL receptor system. *Annu. Rev. Cell Biol.* 1:1–39.
11. Deleted in proof.
12. Hedley, D. W., and E. A. Musgrove. 1986. Transferrin receptor cycling by human lymphoid cells: lack of effect from inhibition of microtubule assembly. *Biochem. Biophys. Res. Commun.* 138:1216–1222.
13. Herman, B., and D. F. Albertini. 1984. A time-lapse video image intensification analysis of cytoplasmic organelle movements during endosome translocation. *J. Cell Biol.* 98:565–576.
14. Hope, M. J., M. B. Bally, G. Webb, and P. R. Cullis. 1985. Production of large unilammellar vesicles by a rapid extrusion procedure. Characterization of size distribution, trapped volume and ability to maintain a membrane potential. *Biochem. Biophys. Acta.* 812:55–65.

15. Hopkins, C. R. 1986. Membrane boundaries involved in the uptake and intracellular processing of cell surface receptors. *Trends Biochem. Sci.* 11: 473–477.
16. Hostetler, K. Y., and P. J. Yazaki. 1979. The subcellular localization of neutral sphingomyelinase in rat liver. *J. Lipid. Res.* 20:456–463.
17. Houslay, M. D., and K. K. Stanley. 1982. Dynamics of Biological Membranes. John Wiley & Sons Inc., New York. 1–330.
18. Kanfer, J. N., O. M. Young, D. Shapiro, and R. O. Brady. The metabolism of sphingomyelin. I. Purification and properties of a sphingomyelin-cleaving enzyme from rat liver tissue. *J. Biol. Chem.* 241:1081–1084.
19. Kishimoto, Y. 1975. A facile synthesis of ceramides. *Chem. Phys. Lipids.* 15:33–36.
20. Kremer, J. M. H., M. W. J. v. d. Esker, C. Pathmamanoharan, and P. H. Wiersema. 1977. Vesicles of variable diameter prepared by a modified injection method. *Biochemistry.* 16:3932–3935.
21. Labarca, C., and K. Paigen. 1980. A simple, rapid and sensitive DNA assay procedure. *Anal. Biochem.* 102:344–352.
22. Lewis, V., S. A. Green, M. Marsh, P. Vihko, A. Helenius, and I. Mellman. 1985. Glycoproteins of the lysosomal membrane. *J. Cell Biol.* 100:1839–1847.
23. Leyva, A., Jr., and W. N. Kelly. 1974. Measurement of DNA in cultured human cells. *Anal. Biochem.* 62:173–179.
24. Lipsky, N. G., and R. E. Pagano. 1984. Fluorescent sphingomyelin labels the plasma membrane of cultured fibroblasts. *Ann. NY Acad. Sci.* 435:306–308.
25. Lipsky, N. G., and R. E. Pagano. 1985. Intracellular translocation of fluorescent sphingolipids in cultured fibroblasts: endogenously synthesized sphingomyelin and glucosylcerebroside analogues pass through the Golgi apparatus en route to the plasma membrane. *J. Cell Biol.* 100:27–34.
26. Lipsky, N. G., and R. E. Pagano. 1985. A vital stain for the Golgi apparatus. *Science (Wash. DC).* 228:745–747.
27. Martin, O. C., and R. E. Pagano. 1987. Transbilayer movement of fluorescent analogs of phosphatidylserine and phosphatidylethanolamine at the plasma membrane of cultured cells. *J. Biol. Chem.* 262:5890–5898.
28. Matteoni, R., and T. E. Kreis. Translocation and clustering of endosomes and lysosomes depends on microtubules. *J. Cell Biol.* 105:1253–1265.
29. Nichols, J. W., and R. E. Pagano. 1981. Kinetics of soluble lipid monomer diffusion between vesicles. *Biochemistry.* 20:2783–2789.
30. Pagano, R. E. 1988. What is the fate of diacylglycerol produced at the Golgi apparatus? *Trends. Biochem. Sci.* 13:202–205.
31. Pagano, R. E. 1989. A fluorescent derivative of ceramide: physical properties and use in studying the Golgi apparatus of animal cells. *Methods Cell Biol.* 29(Pt. A):75–85.
32. Pagano, R. E., and R. G. Sleight. 1985. Defining lipid transport pathways in animal cells. *Science (Wash. DC).* 229:1051–1057.
33. Pagano, R. E., and O. C. Martin. 1988. A series of fluorescent *N*-(acyl)-sphingosines: synthesis, physical properties, and studies in cultured cells. *Biochemistry.* 27:4439–4445.
34. Pavelka, M., and A. Ellinger. 1985. Localization of binding sites for Concanavalin A, *Ricinus communis* I and *Helix pomata* lectin in the Golgi apparatus of rat small intestinal absorptive cells. *J. Histochem. Cytochem.* 33:905–914.
35. Rouser, B., A. N. Siakotos, and S. Fleisher. 1981. Quantitative analysis of phospholipids by thin-layer chromatography and phosphorous analysis of spots. *Lipids.* 1:85–86.
36. Singer, S. J., and A. Kupfer. 1986. The directed migration of eukaryotic cells. *Annu. Rev. Cell Biol.* 2:337–365.
37. Sleight, R. G., and R. E. Pagano. 1984. Transport of a fluorescent phosphatidylcholine analog from the plasma membrane to the Golgi apparatus. *J. Cell Biol.* 99:742–751.
38. Steinman, R. M., I. S. Mellman, W. A. Muller, and Z. A. Cohn. 1983. Endocytosis and the recycling of plasma membrane. *J. Cell Biol.* 96:1–27.
39. Storrie, B., R. R. Pool, Jr., M. Sachdeva, K. M. Maurey, and C. Oliver. 1984. Evidence for both prelysosomal and lysosomal intermediates in endocytic pathways. *J. Cell Biol.* 98:108–115.
40. Struck, D. K., and R. E. Pagano. 1980. Insertion of fluorescent phospholipids into the plasma membrane of a mammalian cell. *J. Biol. Chem.* 255:5404–5410.
41. Struck, D. K., D. Hoekstra, and R. E. Pagano. 1981. Use of resonance energy transfer to monitor membrane fusion. *Biochemistry.* 20:4093–4099.
42. Swanson, J., A. Bushnell, and S. C. Silverstein. 1987. Tubular lysosome morphology and distribution within macrophages depend on the integrity of cytoplasmic microtubules. *Proc. Natl. Acad. Sci. USA.* 84:1921–1925.
43. Uster, P. S., and R. E. Pagano. 1986. Resonance energy transfer microscopy: observations of membrane-bound fluorescent probes in model membranes and in living cells. *J. Cell Biol.* 103:1221–1234.
44. van Meer, G., E. H. K. Stetzer, W. Wijnaendts-van-Resandt, and K. Simons. 1987. Sorting of sphingolipids in epithelial (Madin-Darby canine kidney) cells. *J. Cell Biol.* 105:1623–1635.
45. van Renswoude, J., K. R. Bridges, J. B. Harford, and R. D. Klausner. 1982. Receptor-mediated endocytosis of transferrin and the uptake of Fe in K562 cells: identification of a nonlysosomal acidic compartment. *Proc. Natl. Acad. Sci. USA.* 79:6186–6190.
46. Virtanen, I., P. Ekblom, and P. Laurila. 1980. Subcellular compartmentalization of saccharide moieties in cultured and malignant cells. *J. Cell Biol.* 85:429–434.
47. Yamashiro, D. J., B. Tycko, S. R. Fluss, and F. R. Maxfield. 1984. Segregation of transferrin to a mildly acidic (pH 6.5) para-Golgi compartment in the recycling pathway. *Cell.* 37:789–800.